Oleg I. Shpotyuk [1]
Valentyna O. Balitska [2]

[1] *Pedagogical University, Częstochowa*
[2] *Scientific Research Company Carat, Lvov*

PHYSICAL PECULIARITIES OF ELECTRON-INDUCED DICHROISM IN VITREOUS As_2S_3

Abstract: The effect of dichroism (transmission coefficient difference for sonde light with parallel and perpendicular orientation of the polarization plane) was investigated in vitreous As_2S_3 irradiated by accelerated electrons (E=2,8 MeV) with more than $5 \cdot 10^{15}$ cm $^{-2}$ fluences. *

Detailed investigations of the influence of absorbed light (photoinduced effects) [1,2] and high energy ionizing radiation (radiation-induced effects) [3,4] on amorphous chalcogenide semiconductors (AChS) carried out in recent years reveal the fundamental reason for the similarity between these effects. It has been shown that the microstructural mechanism of both the photo- and radiation--structural transformations is determined by coordination defect formation processes, i.e. induced chemical bond interchange accompanied by relaxation transformations in the structural region of intermediate range ordering [1-6]. This conclusion concerns not only scalar (isotropic physical properties changes), but also vectorial effects of photo- and radiation-induced dichroism revealed under the influence of linear polarized light [7-9] and a beam of accelerated electrons [10,11], respectively.

The effect of electron-induced dichroism (EID) was first observed in vitreous v-As_2S_3, irradiated by accelerated electrons in the orthogonal plane to the direction of a sonde light beam [10,11]. This effect reveals itself as a difference in absorption coefficients for sonde light with parallel and perpendicular orientations of the polarization plane analogous to the well-known photoinduced dichroism [9].

Investigated samples of v-As_2S_3 were synthesized from components of 99.999% purity in evacuated quartz ampoules [10,11]. The temperature of synthesis did not exceed 1050 K. The best samples of homogenization with the absence of internal strained spots were achieved with additional thermal annealing at temperatures of 435-445 K. All investigated samples were in the form of a cube of 6-8 mm rib length and high-quality polished borders.

The irradiation was carried out using directed beam of accelerated electrons of energy 2.8 MeV and more than $\Phi>10^{15}$ cm^{-2} fluences up to $\Phi=5\cdot10^{17}$ cm^{-2} perpendicular to the BB_1C_1C plane (Fig.1). This plane of the v-As_2S_3 cube was denoted by the sign || taking into account collinearity of the normal vector of this plane and direction of the electron beam propagation. The sonde light beam had a diameter close to 2-3 mm and passed through the sample at distance 1.5-2 mm from the irradiated BB_1C_1C plane. Analogously, the ABCD plane of the cube having the normal vector with perpendicular orientation to the electron beam direction was denoted by the sign ⊥. The complete penetration of the accelerated electrons throughout the zone of the sample investigated was achieved under these conditions. The calculated depth of the electron absorption was close to 5-6 mm [12]. Hence, we could distinguish two mutually orthogonal directions for sonde light with parallel aa (||) and perpendicular bb (⊥) polarizations with respect to the direction of the accelerated electrons (Fig.1).

All measurements were performed one day after electron irradiation using a „Specord M-40" spectrophotometer (200-900 nm). The effects produced by inhomogeneity of scalar electron-induced darkening [13] were excluded, changing the direction of sonde propagation by opposite one.

The EID was described by the parameter κ in accordance with the well-known expression [9]:

$$\kappa = \Delta\alpha \cdot d = (\alpha_{II} - \alpha_{\perp}) \cdot d = \frac{2 \cdot (\tau_{\perp} - \tau_{II})}{(\tau_{\perp} - \tau_{II})}$$

where $\alpha_{//}$ ($\tau_{//}$) and $\alpha_{\perp}$ ($\tau_{\perp}$) are the absorption coefficients (transmission coefficients) for sonde light with parallel (aa) and perpendicular (bb) orientations of the polarization plane, and d is the sample thickness.

The spectral dependences of the parameter κ for the v-As_2S_3 cubic samples after electron irradiation by $\Phi=5\cdot10^{16}$ cm^{-2} and subsequent annealing during 2 hours at various temperatures T are shown in Fig.2 (curves 1-5). It should be noted that the EID is observed in the spectral region of optical absorption coefficient edge (see insert to the Fig.2).

Studying the dose dependence of the EID, we have shown that this effect appeared after electron irradiation with $\Phi=5\cdot10^{15}$-10^{16} cm^{-2}, reached the relative maximum in the region of $\Phi=5\cdot10^{15}$-10^{17} cm^{-2} and later slightly increased by 10-15% without saturation up to $\Phi=5\cdot10^{17}$ cm^{-2}.

The main features of EID in the v-As_2S_3 after $\Phi=5\cdot10^{16}$ cm^{-2} fluence of irradiation will now be considered. The sharp edge of the EID is detected at the photon energies $h\nu > 1.9$ eV (Fig. 2, curve 1). The κ value reaches 0.6-0.7, which is greater than the analogous parameter for the photoinduced dichroism [9]. The slope of the $\kappa(h\nu)$ curve is approximately equal to $\sigma=6$-7 $(eV)^{-1}$.

The next thermal annealing produces the blue shift of this curve, as in the case of the restoration of thermally induced optical properties in the γ-irradiated AChS [14]. However, contrary to this process, the thermal bleaching of the EID begins at temperatures higher than 290-300 K and finishes near 420-430 K (Fig. 2, curves 2-5) without sufficient thresholds in this temperature region. The slope σ increases on annealing up to 15-20 eV^{-1}.

The extensive „tail" of the EID is observed in the longer wavelength region ($\kappa<0.10$-0.15). This EID „tail" decreases after annealing, but linear prolongations of these $\kappa(h\nu)$ curves cross through one point F (see Fig. 2). This feature is different in comparison with the analogous scalar radiation-induced darkening effect [3-5,14], associated with a parallel shift of the absorption coefficient spectrum.

We have established that the EID in the v-As_2S_3 decayed completely at T=300 K during 10-15 days, while the photoinduced dichroism decays only partially at this temperature [9].

Hence, the supposition of the external factor influence (reorientation) on the native (created before irradiation) defect centres in the AChS, proposed by authors [9] for the explanation of photoinduced dichroism mechanism, is probably not suitable for our effect. In addition, we think that the microstructural scheme of the photoinduced topological reorientation of preexisting native dipoles in the form of intimate valence-alternation pairs [15], including three rigid covalent bond interchanges [6], will be scarcely probable for the AChS of all chemical compositions. Really the native defect concentration in annealed glasses is very small in comparison with thin films, obtained under the more unbalanced conditions of thermovacuum evaporation [15].

We maintain that the EID mechanism in the AChS is related to electron-induced formation of new oriented (relative to electron flow) defects. The IR Fourier spectroscopy of additional reflectivity in the region of the v-As_2S_3 main vibrational bands - pyramidal As_2S_3 units (335-285 cm^{-1}), molecular products with „wrong" homopolar As-As (379, 340, 231, 210, 168 and 140 cm^{-1}) and S-S

bonds (243 and 188 cm^{-1}) [16-19] is an effective method for the experimental investigation of such defect formation processes [4,5].

Thus, the Fourier spectroscopy measurements were carried out for the microstructural mechanism study of the EID. The IFS-113V „Bruker" device was used for the reflectivity spectra, recording in the region of the vibrational bands of the v-As_2S_3 main structural units (400 to 100 cm^{-1}).

All measurements were carried out for planes of the cube oriented perpendicular (ABCD or $\perp$) and parallel (BB_1C_1C or $||$) to the direction of electron beam propagation (see Fig.1).

Comparing the integrated $R_\perp$ and $R_{||}$ spectra of the v-As_2S_3 just after electron irradiation ($\Phi=5\cdot10^{16}$ cm^{-2}), we note that the background $R_\perp$ value is higher than $R_{||}$. Simultaneously, the vibrational band at 420 cm^{-1} corresponding to As-O complexes [22] is more intensive in the $R_\perp$ spectrum, while vibrational bands in the region 335-285 cm^{-1}, associated with As-S chemical bonds [16-19], are slightly distinguished.

These results indicate that two radiation-structural transformations take place at the surface of the investigated samples:

- firstly, the process of surface damages (reological changes) due to direct bombardment of high energy accelerated electrons (the analogous process was recently studied in [20]);
- secondly, the process of electron-induced surface oxidation due to chemical interaction of the destructed matrix complexes and absorbed oxygen atoms as in the case of γ-induced surface oxidation of the AChS with prolonged irradiation [21].

It is obvious that the first process is more pronounced on the parallel (BB_1C_1C) plane of the v-As_2S_3 cube, whereas the second one - on the perpendicular (ABCD) plane. The first process leads to the decrease of the background reflectivity level ($R_{||}$) and, consequently, prevents correct identification of the structural transformations on this (BB_1C_1C) plane (at least up to temperatures of 390-400 K, when the processes of reological damage treatment begin). The second process (oxidation) does not affect the vibrational spectrum $R_\perp$ of the v-As_2S_3 main structural units (400-100 cm^{-1}) because stretching and bending modes corresponding to the As-O complexes are situated in the ν>400 cm^{-1} region [22,23].

The spectrum of the additional reflectivity $\Delta R_\perp$ (subtracted reflection spectra before and after influence of external factors) for the electron-irradiated ($\Phi=5\cdot10^{16}$ cm^{-2}) v-As_2S_3 induced by thermal annealing at T=333 K is shown in Fig.3. Positive values of $\Delta R>0$ (additional reflectivity) correspond to appearing complexes and negative values of $\Delta R<0$, on the contrary, correspond to disappearing complexes.

We can distinguish more than ten additional reflectivity bands ($\Delta R_{\perp}>0$) corresponding to various structural units of the v-As_2S_3 based on the heteropolar As-S and homopolar As-As and S-S covalent chemical bonds. Hence in accordance with Fig.3, the concentration of the main structural units of the investigated samples is sufficiently increased after thermal annealing, the greatest increase being characteristic for the As-based complexes associated with $\Delta R_{\perp}$ bands in the 335-285 cm^{-1} region [16-19]. This effect is not appropriate to non-irradiated AChS samples annealed at temperatures below T=440-450 K [24].

On decreasing the annealing temperature to T=390-400 K the intensities of the v-As_2S_3 vibrational modes shown in Fig.3 increase, especially those related to the homopolar chemical bonds (379, 340, 243, 231, 188, 168 and 140 cm^{-1}). It permits us to conclude that electron-induced structural defects resulting from the destructed heteropolar As-S bonds are the most unstable and sensitive to thermal treatment.

The one possible outcome of the results presented above is the existence of a certain concentration of broken chemical bonds in the structural network of the electron-irradiated samples. In other words, the 8-N rule is not satisfied in these samples in so far as some of the atoms do not fulfil their normal valency. In accordance with our calculations, the quantity of such atoms indicated by the obtained Fourier spectrum (Fig.3) is equal to 8-9% (estimation on the basis of a comparison of the vibrational band intensities in the 335-285 cm^{-1} before and after electron irradiation). These atoms with unsaturated valencies may be characterized as specific structural defects of the v-As_2S_3 with lower coordination (undercoordinated atoms) [25].

Because the process of chemical bond breaking in the AChS has a homolytical character, i.e. electrons principally forming the covalent bond are localized only at one atom [15], there are no unpaired spins in this process, and created defects are the pairs of undercoordinated atoms with opposite electrical charges. These defects appear in the glassy matrix due to displacements of the covalently bonded atoms on bombardment by high energy accelerated electrons in accordance with the overthreshold mechanism [26]. The coincidence of the calculated concentration of such displaced atoms [24] and the above mentioned defects estimated from our experimental results (Fig.3) is in support of this explanation.

These defects are preferentially oriented along the direction of the electron beam propagation and, as a result, can be considered as oriented electrical dipoles producing the observed EID. At higher temperatures (over 390-400 K) the obtained signal of additional reflectivity has a more complex

shape. We can distinguish two components in the thermally induced $\Delta R_{\perp}$ spectrum:

1) a component analogous to that shown in Fig.3 with more intensive vibrational bands in the region corresponding to homopolar chemical bonds,
2) a component of the chemical bond interchange process connected with the thermal annihilation of coordination defects (As_4^+, S_1^-) at the reversible stage of scalar radiation-structural transformations which have been described in detail in [3-5].

The second component appears only under thermal annealing at temperatures over the restoring threshold (390-400 K) [14]. It must be noted that under these conditions the reological electron-induced damage at the perpendicular BB_1C_1C plane only partly disappears and the background reflectivity $R_{||}$ of this plane increases (this result can be noticed visually from restoration of the specific shine). However, the exact quantitative estimation of both components of the additional reflectivity is difficult because of their overlapping.

The EID is fully bleached on thermal annealing near T=420–430 K, when both the $\Delta R_{\perp}$ and $\Delta R_{||}$ spectra are saturated. The final concentration of the undercoordinated atoms (with respect to the total concentration of the atoms) annihilated at this temperature is approximately 10-12% in accordance with our estimation for the vibrational band in the 335–285 cm^{-1} region.

Using the model of the v-As_2S_3 random structural network [15], we conclude from our experimental results (see Fig.3) that defects indicated as undercoordinated atoms are (As_2^+, S_1^-), (As_2^-, As_2^+), and (S_1^-, S_1^+). The charge of the defect centre is denoted by a superscript and the quantity of nearest neighbour atoms by a subscript. They appear in the structural matrix by pairs preserving the electroneutrality of the sample. Such defects are quite stable just after irradiation at room temperature and unstable at high temperatures in accordance with our experimental data.

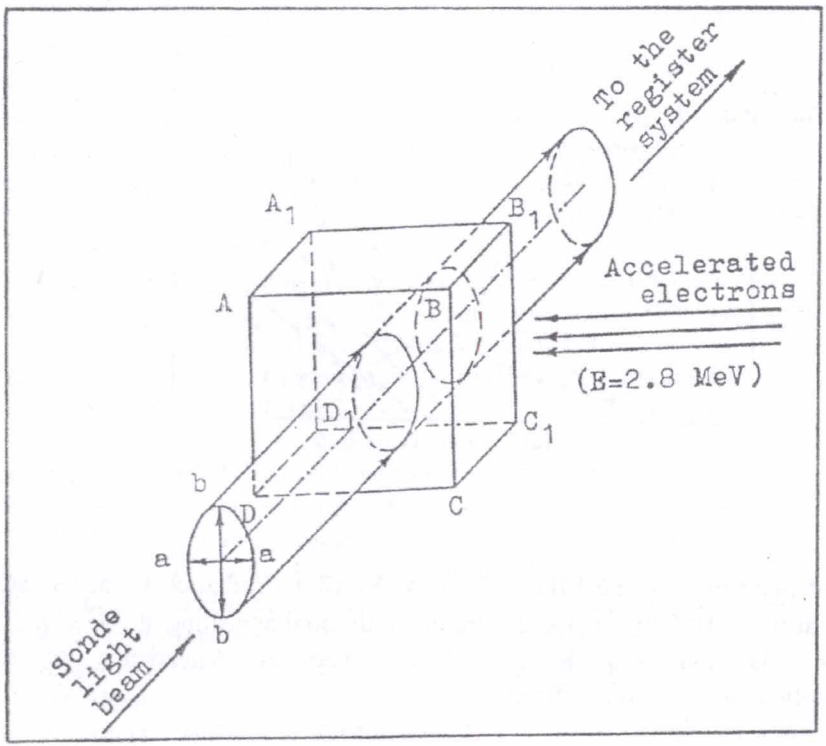

Fig. 1.
Scheme illustrating the experimental procedure for the EID observation in the v-As_2S_3 cube

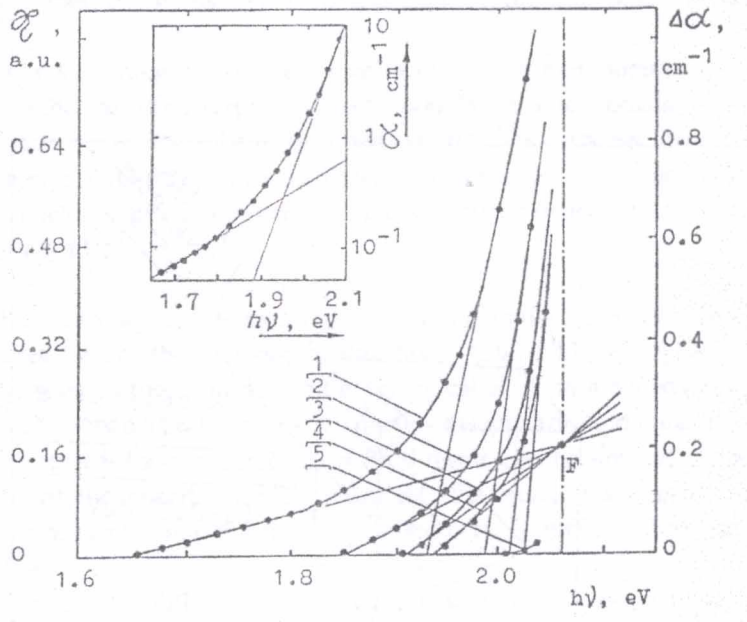

Fig.2.
Spectral dependences of the EID in the v-As_2S_3 after irradiation by accelerated electrons at $\Phi=5 \cdot 10^{16}$ cm^{-2} (1) and subsequent thermal annealing at 343 (2), 373 (3), 398 (4) and 423 K (5). Insert: spectral dependence of the v-As_2S_3 optical absorption coefficient

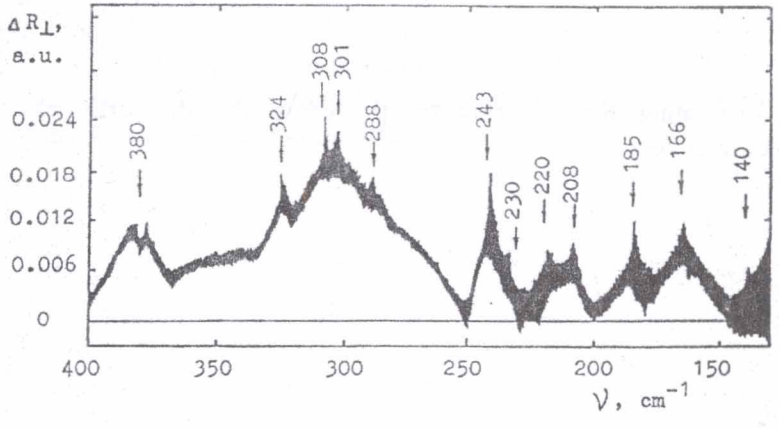

Fig. 3
Spectrum of the additional reflectivity $\Delta R_\perp$ of the electron-irradiated v-As_2S_3 by thermal annealing at 333 K

REFERENCES

1. S.R. Elliot, *J. Non-crystall. Solids* 1986, **81**, 71
2. H. Frizsche, *Phil. Mag.* 1993, **68**, 561
3. O.I. Shpotyuk, A.O. Matkovskii, *J. Non-crystall. Solids* 1994, **176**, 45
4. O.I. Shpotyuk, *Phys. stat. Sol.A* 1994, **145**, 69
5. O.I. Shpotyuk, *Phys. stat. Sol. B.* 1994, **183**, 365
6. S.R. Elliott, V.K. Tikhomirov, *J. Non-crystall. Solids* 1995, **198-200**, 669
7. V.K. Malinovsky, V.C. Zhdanov, *J. Non-crystall. Solids* 1982, **52**, 31
8. R. Grigorovici, A. Vancy, L. Chita, *J. Non-crystall. Solids* 1983, **59-60**, 909
9. V.M. Lyubin, V.K. Tikhomirov, *Fiz. tverd. Tela* 1991, **33**, 2063
10. O.I. Shpotyuk, *Ukr. fiz. Zh.* 1993, **8**, 1484
11. O.I. Shpotyuk, V.O. Balitska, *Zh. prikl. Spektroskopii* 1994, **63**, 566
12. A.K. Pikaev, *Modern Radiation Chemistry. Basic Principles, Experimental Technique and Methods*, Nauka, Moscow 1985, 374
13. R.M. Guralnic, S.S. Lantratova, V.M. Lyubin, S.S. Sarsembinov, *Fiz. tverd. Tela* 1982, **24**, 1334
14. O.I. Shpotyuk, *Zh. prikl. Spektroskopii* 1987, **46**, 122
15. M.H. Brodsky. *Amorphous Semiconductors,* Mir, Moscow 1982, 419
16. D.W. Scott, J.P. McCullough, F.H. Kruse, *J. Molec. Spectroscopy* 1964, **13**, 313
17. S.A. Solin, G.N. Papatheodorou, *Phys. Rev.B.* 1977, **15**, 2084
18. U. Strom, T.P. Martin, *Solid State Commun.* 1979, **29**, 527
19. T. Mori, K. Matsuishi, T. Arai, *J. Non-crystall. Solids* 1984, **65**, 269
20. K. Tanaka, *Abstr. of NATO ARW „Physics and Applications of Non-Crystalline Semiconductors in Optoelectronics"*, Chisinau, Moldova, 1996, 29
21. O.I. Shpotyuk, *Ukr. fiz. Zh.* 1987, **23**, 509
22. I.I. Rosola, P.P. Puga, V.V. Chiminies, D.V. Chepur, *Ukr. fiz. Zh.* 1981, **26**, 1875
23. J.A. Savage, *J. Non-crystall. Solids* 1982, **47**, 101
24. A.O. Matkovsky, S.B. Ubizsky, O.I. Shpotyuk, *Fiz. tver. Tela* 1990, **6**, 1790
25. V.N. Kornelyuk, *Visnyk Lviv. Univers., Ser. fiz.* 1989, **22**, 92
26. M.I. Klinger, *Izv. AN Latv. SSR, Ser. fiz. i techn. Nauk* 1987, **4**, 58

* **Vth International Seminar on Physics and Chemistry of Solids, Złoty Potok - Częstochowa, May 1999**

Oleg I. Shpotyuk
Valentyna O. Balitska

Fizyczne osobliwości elektronowo indukowanego dichroizmu w szklistym As_2S_3

Streszczenie: Badano elektronowo indukowany dichroizm (różnica współczynnika przepuszczania światła o równoległej i prostopadłej orientacji płaszczyzny polaryzacji) szklistego As_2S_3 przy napromieniowaniu przyspieszonymi elektronami (E = 2,8 MeV) o strumieniu powyżej $5 \cdot 10^{15}$ cm^{-2}.